Accepted Manuscript

Binding of LcrV protein from Yersinia pestis to human T-cells induces apoptosis, which is completely blocked by specific antibodies

Vyacheslav M. Abramov, Igor V. Kosarev, Vladimir L. Motin, Valentin S. Khlebnikov, Raisa N. Vasilenko, Vadim K. Sakulin, Andrey V. Machulin, Vladimir N. Uversky, Andrey V. Karlyshev

PII: S0141-8130(18)33519-0
DOI: doi:10.1016/j.ijbiomac.2018.09.054
Reference: BIOMAC 10489

To appear in: *International Journal of Biological Macromolecules*

Received date: 10 July 2018
Revised date: 11 September 2018
Accepted date: 11 September 2018

Please cite this article as: Vyacheslav M. Abramov, Igor V. Kosarev, Vladimir L. Motin, Valentin S. Khlebnikov, Raisa N. Vasilenko, Vadim K. Sakulin, Andrey V. Machulin, Vladimir N. Uversky, Andrey V. Karlyshev , Binding of LcrV protein from Yersinia pestis to human T-cells induces apoptosis, which is completely blocked by specific antibodies. Biomac (2018), doi:10.1016/j.ijbiomac.2018.09.054

Binding of LcrV protein from *Yersinia pestis* to human T-cells induces apoptosis, which is completely blocked by specific antibodies

Vyacheslav M. Abramov,[a] Igor V. Kosarev,[a] Vladimir L. Motin,[b] Valentin S. Khlebnikov,[a] Raisa N. Vasilenko,[a] Vadim K. Sakulin,[a] Andrey V. Machulin,[c] Vladimir N. Uversky,[d,e,*] and Andrey V. Karlyshev[f]

[a] *Department of Immunology and Biodefence, Institute of Immunological Engineering, 142380 Lyubuchany, Russia;*

[b] *Department of Pathology/Microbiology & Immunology, University of Texas Medical Branch, Galverston, Texas 77555, USA;*

[c] *Skryabin Institute of Biochemistry and Physiology of Microorganisms, Russian Academy of Sciences, Pushchino 142290, Russia;*

[d] *Department of Molecular Medicine, Morsani College of Medicine, University of South Florida, Tampa, Florida 33612, USA;*

[e] *Institute for Biological Instrumentation, Russian Academy of Sciences, Pushchino 142290, Russia;*

[f] *Department of Science, Engineering and Computing, Kingston University, Kingston, UK.*

*** Corresponding author**: VNU, E-mail: vuversky@health.usf.edu; Phone: 8139745816; Fax: 8139747357

KEYWORDS. Yersinia; LcrV protein; plague; interferon-γ; apoptosis.

ABSTRACT. The V antigen (LcrV) of the plague bacterium *Yersinia pestis* is a potent protective protein that is considered as a vaccine component for humans. LcrV mediates the delivery of Yop toxins into host cells and upregulates TLR2-dependent IL-10 production. Although LcrV can interact with the receptor-bound human interferon-γ (hIFN-γ), the significance of these interactions in plague pathogenesis is not known. In this study, we determined the parameters of specific interactions of Lcrv and $LcrV_{68-326}$ with primary human thymocytes and Jurkat T-leukemia cells in the presence of receptor-bound hIFN-γ. Although the C-terminal region of hIFN-γ contains a $GRRA_{138-141}$ site needed for high-affinity binding of LcrV and $LcrV_{68-326}$, in the hIFN-γ homodimer, these $GRRA_{138-141}$ target sites becomes accessible for targeting by LcrV or $LcrV_{68-326}$ only after immobilization of the hIFN-γ homodimer on the hIFN-γ receptors of thymocytes or Jurkat T-cells. The interaction of LcrV or $LcrV_{68-326}$ with receptor-bound hIFN-γ on the thymocytes or Jurkat T-cells caused apoptosis of both cell types, which can be completely blocked by the addition of monoclonal antibodies specific to the $LEEL_{32-35}$ and $DEEI_{203-206}$ sites of LcrV. The ability of LcrV to utilize hIFN-γ is insidious and may account in part for the severe symptoms of plague in humans.

1. Introduction

The plague caused by *Yersinia pestis* is the most devastating bacterial infection known to man [1]. *Y. pestis* recently evolved from *Yersinia pseudotuberculosis*, which diverged from *Yersinia enterocolitica* about 50 million years ago [2]. All three species share an ~70-kb plasmid (termed pCD in *Y. pestis* [3] and pYV in enteropathogenic *Y. pseudotuberculosis* and *Y. enterocolitica*) that encodes the V antigen (LcrV), yersiniae outer proteins (Yops), and an attendant type 3

secretion system (T3SS). The functions of T3SS are activated by pCD/pYV-encoded LcrF (VirF in enteropathogenic yersinia) [4] at 37ºC [5] and expressed upon host cell contact [6] or residence in Ca^{2+}-deficient medium [7] and host fluids [8]. The most important feature of the plague is that it is a rapidly progressing disease, suggesting that *Y. pestis* prevents the activation of the innate immune response to infection as first shown for pCD-dependent downregulation of proinflammatory cytokines [9]. LcrV is a multifunctional protein and serves as a major regulator and effector of virulence. At the first stage of plague pathogenesis, LcrV acts as a short-term weapon of *Y. pestis* [10, 11]. LcrV forms a tip on the YscF nanotube of T3SS injectosome [12] and mediates translocation of Yop effectors into the target cells [13] for the initiation of bacterial growth in host organs and the buildup of bacterial cells that release sufficient amounts of secreted LcrV to induce effective levels of interleukin 10 (IL-10) at the next stage of pathogenesis, when it acts as a long-term weapon for *Y. pestis* [10, 11, 14]. This strategy also involves the production of noninflammatory lipopolysaccharide [15], degradation of those Yops that fail to undergo translocation into the host cell cytoplasm [16], inhibition of host MAPK kinase and NF-kB pathways by YopJ, resulting in apoptosis of professional phagocytes [17-19], and induction of mitochondrial-dependent apoptosis of T-cells by YopH [20] or by YpkA [21]. Deletion of YopJ did not result in decreased virulence of *Y. pestis*, systemic spread, or colonization levels in the spleen and blood [22]. At the same time, deletion of LcrV converted virulent strains of *Y. pestis* into avirulent ones [23, 24]. Although antibodies to Yop proteins could be found in the sera of both people and animals that survived a plague infection or were vaccinated with live plague vaccine, their protective potential is insufficient to be used in a subunit vaccine [25]. In contrast, the passive transfer of both LcrV-specific polyclonal or monoclonal antisera protected experimental animals against bubonic and pneumonic plague [23,

24, 26-32]. Sub-unit vaccines based on LcrV or LcrV+F1 proteins provided a high degree of protection in mice, guinea pigs, and nonhuman primates [33-41].

Y. pestis replicates whiting lymphoid tissues. Because LcrV derivatives and anti-LcrV antibodies are being developed for prevention and prophylaxis against plague in humans, it is important to better understand the detailed mechanisms of all effects of LcrV, their relative importance in plague pathogenesis and inhibiting of Yops effects, such as the target-cell killing of human T lymphocytes prevented by anti-LcrV antibodies. Earlier we demonstrated that LcrV possesses two non-cooperative binding domains ($LEEL_{32-35}$ and $DEEI_{203-206}$) capable of recognizing human IFN-γ but not mouse IFN-γ bound to its receptors (IFN-γ R-IFN-γ) on human U-937 cells and human alveolar macrophages [42]. Human IFN-γ, but not mIFN-γ, possessed a $GRRA_{138-141}$ site on the C-terminus of the molecule responsible for the high-affinity specific binding of LcrV [42]. The purpose of the present study was to obtain information regarding the specificity and avidity of the interaction between LcrV and hIFN-γ bound to its receptors on the surface of human primary thymocytes and Jurkat T-leukemia cells. We show here that LcrV uses receptor-bound hIFN-γ for initiation of apoptosis of human T-cells. Monoclonal anti-LcrV antibodies completely blocks the programmed death of human T-cells induced by LcrV and $LcrV_{68-326}$.

Materials and Methods

Recombinant Proteins

LcrV (defined in Figure 1A) was produced as described previously [42] using *lcrV* encoded within the *lcrGVH-yopBD* operon of pCD1 from the *Y. pestis* strain KIM [43]. After amplification with PCR using sites for *Eco*RI and *Bam*HI, *lcrV* was inserted into the vector

pRSET A (Invitrogen, Carlesbad, CA) opened with *Bam*HI and *Eco*RI. This construct, expressed in *Escherichia coli* BL21(DE3), encoded N-terminal hexahistidine, an enterokinase cleavage site, and then LcrV in its entirety. Similar engineering of *E. coli* BL21(DE3) transformed with pVHB62 encoding $LcrV_{68-326}$ has been described [36]. LcrV and $LcrV_{68-326}$ encoded by these constructs were induced by IPTG, purified to homogeneity by Ni-affinity chromatography, and then freed of hexahistidine by treatment with enterokinase [36]. Homogeneous dimers of LcrV and $LcrV_{68-326}$ were purified by gel-filtration on Sepharose CL-4B column (Sigma Chemical Co., St. Louis, MO). Endotoxin was removed from the preparations of purified protein using polymyxin B-agarose (Sigma). Endotoxin-depleted preparations contained 0.16 ± 0.03 pg (mean ± SE, n =5) of endotoxin/μg of protein as measured by the *Limulus* amebocyte lysate assay system. Preparations of recombinant human IFN-γ (antiviral activity of 2.0×10^7 U/mg) and C-terminally truncated hΔIFN-γ (antiviral activity 1.5×10^7 U/mg) lacking six C-terminal amino acids as defined in Figure 1C and mouse IFN-γ were kindly supplied by Dr. V. Fedyukin (JSC "ImmunoPharm", Obolensk, Russia). Circular dichroism spectra of hIFN-γ and hΔIFN-γ were almost identical. Highly purified human IFN-α2 was purchased from PeproTech, Ltd. (London, U.K.). Purity of recombinant proteins was monitored by SDS-PAGE and silver staining [44].

Synthetic Peptides

Derivatives of LcrV (Figure 1B) were synthesized as described [42] using a solid-phase model 9500 peptide synthesizer (Biosearch Technologies, Inc., Novato, CA) and purified by HPLC chromatography. The purity and sequence of these peptides were confirmed by amino acid analysis and mass spectrometry.

Cell Cultures and Growth Conditions

Normal human thymocytes were obtained from children aged up to 4 months that underwent thymus removal during cardiac surgery (Cardiocenter, Moscow, Russia). During the period of our studies, Cardiocenter had a protocol approved by its ethical committee for the surgical treatment of congenital heart diseases, according to which, in order to get the access to the heart, a part of the sternum was removed along with a part of the thymus. After performing a heart surgery, the post-surgical material was disposed. The study of the properties of thymocytes isolated from post-surgical material was approved by the ethical committee of Cardiocenter and Ethical Committee of the Institute of Immunological Engineering. Suspension of individual cells was obtained via thymus disintegration and following purification using gradient centrifugation in Ficol Hypaqu. Thymocytes were washed thrice in an RPMI 1640 medium containing 2% fetal calf serum (FCS). Cell vitality was determined using methylene blue and reached 98% [45]. Jurkat T-leukemia cells were kept at logarithmic growth in TPMI 1640 medium supplemented with 10% FCS, 2 mM L-glutamin,1 mM sodium pyruvate, nonessential amino acids and 100 unit/ml each penicillin G and streptomycin.

Monoclonal Mouse Anti-LcrV Antibodies

Peptides from $LcrV_{31-50}$ and $LcrV_{193-210}$ (defined in Figure 1B), which contained active sites LEEL and DEEI responsible for the binding to human IFN-γ, were resynthesized for including a C-terminal cysteine and conjugated to keyhole limpet hemocyanin (KLH) through this additional residue. The peptide-carrier conjugates were purified by gel-filtration and used for elaboration of mouse monoclonal antibodies.

Polyclonal Rabbit Anti-LcrV and Anti-hIFN-γ Antibodies

Human IFN-γ and LcrV protein were adsorbed to aluminum hydroxide. The conjugates were used for the immunization of rabbits. Two groups of rabbits up to 3 animals (chinchilla, 2.5 kg) in each group were used for immunization and obtaining anti-hIFN-γ and anti-LcrV sera. The titer of rabbit sera for hIFN-γ and LcrV had an average value of 500,000. Polyclonal anti-hIFN-γ and anti-LcrV antibodies were elaborated by chromatography on the protein A-Cepharose column.

Radiolabeling of Ligands

^{125}I-LcrV and ^{125}I- $LcrV_{68-326}$ (all 0.09 mCu/μg), as well as iodinated hIFN-γ, hΔIFN-γ, mIFN-γ, and hIFN-α2 (all 0.1 mCu/μg) were prepared with Iodo-Gen (Pierce, Rockford, IL) [46] and ^{23}Na^{125}I and then separated by chromatography on the Sephadex G-25 column.

Binding of the Radioactive Ligands the Cells

Normal human thymocytes or Jurkat T-leukemia cells were collected, washed three times with RPMI-1640 medium, and then adjusted to a concentration of 10^7 per mL of the same medium. Radioactive ligands were then added to individual cultures (total volume of 300 μL), which were then incubated for either 1 h at 4°C or 15 min at 37°C. Thereafter, 50 μL of the cell culture was layered on 250 μL of an *n*-dibutylphthalate/bis (2-ethylhexyl)-phthalate mixture (1:1 v/v) and centrifuged for 2 min at 14,000 *g*. Radioactivity in the resulting precipitate was measured using a model 1275 MINI GAMMA counter (LKB WALLAC, Sweden). Nonspecific binding of radioactive ligands to cells or plastic plates was determined by incubation in 10,000-fold excess of corresponding unlabeled ligand and was equal to 25-27% of the total (specific plus

nonspecific) binding. Results were expressed as the (mean ±SEM, n= 3) in molarity, from which nonspecific binding was subtracted. An essentially identical procedure was used to determine dissociation constants of radioactive LcrV and radioactive $LcrV_{68-326}$ from hIFN-γ immobilized on PVC flat bottom 96 multi-well plates.

Apoptotic Activity of LcrV

LcrV-induced apoptosis of human thymocytes and Jurkat T-leukemia cells was measured by determining light scattering and red fluorescence as described earlier [47]. Thymocytes were cultivated for 24 h as described above and then exposed to LcrV with or without hIFN-γ followed by continued incubation for another 24 h. The cells were then fixed with 70% ethanol to permeabilize the cell membrane and suspended into PBS containing triton-100 (Sigma). Propidium iodide (Sigma) diluted in PBC (containing 0.1% triton X-10 and 0.1% sodium citrate) was then added to this preparation to yield a final concentration of 0.05 mg/ml. Analysis was undertaken with a FACS Calibur Fluid Cytofluorimeter (Becton-Discinson, USA with argon laser (488 nm wavelength) using forward and side light scattering). Red fluorescence was evaluated by propidium iodide for 10,000 cells and expressed in histograms as peak M1 (which is the hypodiploid peak in percent that characterizes apoptotic cells in which DNA is fragmented, and as a result, after washing of these cells, they contain an amount of DNA below the diploid chromosome <2N), peak M2 (which is the diploid peak in percent that characterizes the resting cells in the phase G0 and the cells that are in the presynthetic phase of the G1 cell cycle and which contain the amount of DNA corresponding to the diploid set of chromosomes of 2 N), and peak M3 (a proliferation peak in percentage that characterizes the proliferative potential of cells

in the pre-intolerant phase of G2 and mitosis phase M when the number of chromosomes and the DNA content is doubled by 4N). Data analysis was conducted using the CELLQUEST software.

Computational analysis of intrinsic disorder propensity

The amino acid sequence of human IFN-γ protein was used for the sequence-based analysis of intrinsic disorder predisposition. The per-residue intrinsic disorder of the protein was evaluated by several commonly used disorder predictors, such as PONDR® VLXT [48], PONDR® VSL2 [49], PONDR® VL3 [50], PONDR® FIT [51], and IUPred [52]. These tools were selected based on their specific features. PONDR® VSL2 [49] is one of the more accurate stand-alone disorder predictors [49, 53, 54]. PONDR® VL3 is characterized by high accuracy for predicting long intrinsically disordered regions [55], and PONDR® VLXT is known to have high sensitivity to local sequence peculiarities and can be used for identifying disorder-based interaction sites [56]. IUPred was designed to recognize intrinsically disordered protein regions (IDPRs) from the amino acid sequence alone based on the estimated pairwise energy content [52, 57]. Finally, the metapredictor PONDR® FIT is more accurate than each of its component predictors (PONDR® VLXT [56], PONDR® VSL2 [49], PONDR® VL3 [50], FoldIndex [58], IUPred [52], and TopIDP[59]) [51]).

Results

The human IFN-γ molecule is a noncovalent homodimer that consist of two identical 17-kDa polypeptide chains [60]. The crystal structure of hIFN-γ confirmed its dimeric nature and revealed that two polypeptides self-associate in an antiparallel fashion, producing a molecule that exhibits a two-fold axis of symmetry [61]. Only the homodimeric form of hIFN-γ demonstrates

full biological activity [62]. In our experiments, we used LcrV as a non-covalent homodimer that consist of two identical 35.8 kDa polypeptide chains and $LcrV_{68-326}$ as a non-covalent homodimer that consist of two identical 28.5 kDa polypeptide chains (data not shown). Radioactive ^{125}I-LcrV and ^{125}I- $LcrV_{68-326}$ (defined in Figure 1A) did not interact with hIFN-γ and hΔIFN-γ (the amino acid sequences of C-terminal regions of these proteins are shown in Figure 1C) immobilized on the surface of plastic plate (Table 1). Radioactive ^{125}I- hIFN-γ and ^{125}I-hΔIFN-γ did not interact with LcrV and $LcrV_{68-326}$ immobilized on the surface of plastic plate (Table 1). These results provide strong evidence that LcrV and $LcrV_{68-326}$ do not interact with hIFN-γ and hΔIFN-γ in the used experimental model, where one of the potential partners is immobilized on the surface of the plastic plate. In the next series of experiments, we used Jurkat T-leukemia cells and normal primary human thymocytes for immobilization of hIFN-γ and hΔIFN-γ on the surface of IFN-γ receptors expressed on these cells. Labeled ^{125}I-hIFN-γ and ^{125}I-hΔIFN-γ were bound to IFN-γ receptors on the surface of Jurkat T-cells at low K_d values of (3.6± 0.5)×10^{-10} M and (7.8±0.4) ×10^{-10} M, respectively (Table 2). The C-terminal regions of recombinant hIFN-γ, hΔIFN-γ, and mIFN-γ contain the KRKRS amino acid sequence (Figure 1C) responsible for the high-affinity binding to IFN-γR [63, 64]. However, only hIFN-γ but not hΔIFN-γ and mIFN-γ contains the GRRA amino acid sequence in its C-terminal region (Figure 1C). This motif is responsible for the high-affinity interactions with LcrV or $LcrV_{68-326}$ [42]. Labeled ^{125}I-LcrV alone and labeled ^{125}I-$LcrV_{68-326}$ alone did not bind to the Jurkat T-cells (Table 2). However, labeled ^{125}I-LcrV and ^{125}I-$LcrV_{68-326}$ were able to bind to Jurkat T-cells only in the presence of hIFN-γ, but not in the presence of hΔIFN-γ or anti-LcrV monoclonal antibodies (MABs). K_d values of interactions between Jurkat T-cells and labeled ^{125}I-LcrV or labeled ^{125}I-$LcrV_{68-326}$ in the presence of hIFN-γ were (5.2±0.3)×10^{-10} M and (4.6±0.4)×10^{-10} M, respectively

(Table 2). Labeled ^{125}I- hIFN-γ, ^{125}I-hΔIFN-γ, ^{125}I-hIFN-α2, and ^{125}I-mIFN-γ were bound to the receptors on the surface of human primary thymonocytes at low K_d values of $(4.8\pm0.3)\times10^{-10}$ M, $(6.7\pm0.5)\times10^{-10}$ M, $(5.0\pm0.4)\times10^{-10}$ M, and $(2.9\pm0.2)\times10^{-10}$ M, respectively (Table 3). Labeled ^{125}I-LcrV alone and labeled ^{125}I-$LcrV_{68\text{-}326}$ alone did not bound to human thymocytes (Tables 3 and 4). Labeled ^{125}I-LcrV and ^{125}I-$LcrV_{68\text{-}326}$ were able to bind to human thymocytes in the presence of hIFN-γ, but not in the presence of hΔIFN-γ, hIFN-α2, mIFN-γ or anti-LcrV MABs (Tables 3 and 4). K_d values of interactions between thymocytes and labeled ^{125}I-LcrV or labeled ^{125}I-$LcrV_{68\text{-}326}$ in the presence of hIFN-γ were $(2.7\pm0.6)\times10^{-10}$ M and $(3.5\pm0.4)\times10^{-10}$ M, respectively (Tables 3 and 4). LcrV alone and hIFN-γ alone did not induce apoptosis in Jurkat T-cells (Figure 2 A, B). At simultaneous addition of LcrV and hIFN-γ into the culture medium, the hypodiploid peak was increased, reflecting the induction of apoptosis in Jurkat T-cells (Figure 2C) in comparison to the experiments where LcrV alone (Figure 2A) or hIFN-γ alone (Figure 2B) were added into the medium. The diploid peak and proliferation peak were considerably lower (Figure 2C) in comparison to the experiments, where LcrV alone (Figure 2A) or hIFN-γ alone (Figure 2B) were added into the medium. LcrV alone or $LcrV_{68\text{-}326}$ alone and hIFN-γ alone did not induced apoptosis in human thymocytes (Tables 5 and 6). The addition of LcrV or $LcrV_{68\text{-}326}$ together with hIFN-γ but not with hΔIFN-γ, hIFN-α2, or mIFN-γ in medium induced apoptosis in human thymocytes (Tables 5 and 6). In the presence of LcrV or $LcrV_{68\text{-}326}$ and hIFN-γ, apoptosis reached 45-50%.

Monoclonal antibodies specific to the $LEEL_{32\text{-}35}$ and $DEEI_{203\text{-}206}$ binding sites of Lcrv (these sites are responsible for the interaction with the $GRRA_{138\text{-}141}$ binding site of hIFN-γ) completely blocked programmed cell death induced by LcrV and $LcrV_{68\text{-}326}$ in the presence of hIFN-γ (Tables 5 and 6). Together, all these results show that LcrV and $LcrV_{68\text{-}326}$ in the presence of

hIFN-γ bound to hIFN-γ receptors are potent activators of programmed cell death in both Jurkat T-cells and human primary thymocytes. More importantly, treatment of cells with monoclonal antibodies against $LEEL_{32-35}$ and $DEEI_{203-206}$ binding sites of LcrV completely blocks the programmed death induced by LcrV or $LcrV_{68-326}$.

Discussion

To assess the protective properties of new anti-plague vaccines for humans, mice are most often used as a relevant model organism. The terminal murine plague is an anti-inflammatory disease [9], and LcrV contributes to this process [14] by upregulating IL-10 [65, 66], a powerful anti-inflammatory cytokine that prevents expression of a variety of host inflammatory factors [67, 68]. The obtained results indicate that LcrV and $LcrV_{68-326}$ can efficiently interact with the hIFN-γ immobilized on the IFN-γ receptors of Jurkat T-cells or human thymocytes, but not with the hIFN-γ in solution or with the hIFN-γ immobilized on plastic plates. These observations suggest that the two binding sites $GRRA_{138-141}$ responsible for interaction of the hIFN-γ homodimers with LcrV and $LcrV_{68-326}$ are not accessible in solution or after immobilization of hIFN-γ homodimers on the plastic plates. In contrast, the binding sites $LEEL_{32-35}$ and $DEEI_{203-206}$ on the LcrV molecule are accessible in solution [69].

The crystal structure of a complex between human IFN-γ homodimer and two extracellular domains of soluble IFN-γ receptor α-chains was resolved [70, 71]. Figure 3A represents structure of this complex and show that each IFN-γ monomer contacts one soluble receptor α-chain. As a result, an IFN-γ homodimer serves as a linker between the two IFN-γ receptor α-chains (IFN-γRα-chains). According to Walter and colleagues [70], each protomer of the IFN-γ homodimer consists of six helices (A, B, C, D, E, and F) related by a non-crystallographic twofold axis.

Figure 3B shows that the human IFN-γ homodimer is characterized by a highly intertwined structure, where two C-terminal α-helices (E and F) of one protomer interact with the helices A, B, C, and D of another protomer. It was also pointed out that the 13 residue-long AB loop of one protomer encircle the α-helix F of another protomer [70, 71]. Also, in both protomers, the main chain after the α-helix F (after residue 122) extends to the solvent away from the protein molecule [70]. Overall, it was pointed out that the dimeric structure of human IFN-γ is stabilized by the intertwining of helices across the subunit interface with multiple intersubunit interactions [61]. Such intertwined structure of the homodimer suggests that it is formed as a result of binding-induced folding [72-74]. In other words, it seems that the human IFN-γ is not stable in its monomeric form. In agreement with this hypothesis, Figure 3C shows the results of the intrinsic disorder propensity analysis of this protein by a set of commonly used disorder predictors, PONDR® VLXT, PONDR® VL3, PONDR® VSL2, PONDR® FIT, IUPred_short, and IUPred_long. This analysis suggested that the C-terminal half of human IFN-γ is indeed characterized by high intrinsic disorder predisposition, and the C-tail of this protein (approximately the last 20 residues) is entirely disordered (see Figure 3C). However, it is known that the intrinsically disordered proteins or proteins with intrinsically disordered regions are frequently involved in protein-protein interactions and molecular recognitions [56, 75-87] and undergo at least partial disorder-to-order transitions upon binding [56, 79, 87-94]. These observations were utilized to develop computational tools for the identification of potential disorder-based binding sites. Application of one of such tools, the ANCHOR algorithm [95, 96], revealed that human IFN-γ contains several such potential binding sites, including C-terminally located regions spanning residues 113-117 and 135-136. These observations are in agreement

with the results of earlier investigations showing that the C-terminal region of human IFN-γ is important for biological activity of this protein [63, 64].

Comparison of the crystal structures of IFN-γ homodimer alone (PDB ID: 1HIG) [61], or in complex with two extracellular domains of soluble IFN-γ receptor α-chains was resolved (PDB ID: 1FG9) [70, 71], or complexed with the IFN-γ-binding protein from Ectromelia virus (ECTV) (IFN-γBP_{ECTV}; PDB ID: 3BES) [97] revealed that although interaction with these partners virtually did not affect the structure of the "body" of the IFN-γ molecule, the C-terminal tail underwent noticeable structural changes (see Figure 3D). In fact, in the resolved crystal structure of the IFN-γ homodimer alone (PDB ID: 1HIG) [61], the C-tail contains only the residues AELSPA, whereas the major part of the C-terminal region (residues AKTGKRKRSQMLFRGRRASQ) is absent (see blue structure in Figure 3D), despite the fact that the full-length mature protein was used in these crystallization experiments. The fact that the C-terminal residues are not visible in the corresponding crystal structure (i.e., represent a missing electron density region) indicates their high conformational flexibility. In a complex of the human IFN-γ homodimer with two extracellular domains of IFN-γR α-chains (PDB ID: 1FG9) [70, 71], the resolved structure of the IFN-γ C-tail is extended to include residues AELSPAAKT (see red structure in Figure 3D), whereas the remaining part of C-tail is still missing. Finally, complexation with IFN-γBP_{ECTV} (PDB ID: 3BES) [97] caused the most noticeable structuration of the IFN-γ C-tail, since in this complex, the resolved structure of this region includes residues AELSPAAKTGKRKRS, where an additional short α-helix is formed (see green structure in Figure 3D). These data clearly indicate that the peculiarities of structural organization of the C-tail of human IFN-γ depend strongly on a binding partner. Therefore, based on the analysis of the available structural information, one can hypothesize that, after interaction of the human IFN-γ

homodimer with two IFN-γR α-chains, some conformational changes take place in the IFN-γ homodimer, as a result of which two $GRRA_{138-141}$ binding sites localized at the C-terminal ends of the human IFN-γ homodimer accommodate a structure suitable for interaction with LcrV and $LcrV_{68-326}$ homodimers. The appearance of two binding cites for LcrV or $LcrV_{68-326}$ homodimers on IFN-γ homodimer after the formation of the [IFN-γR α-chains-IFN-γ homodimer] complex is shown by arrows on Figure 3A.

The IFN-γ receptor α-chain is expressed at moderate levels on the surfaces of nearly all cells of the human organism, being especially abundantly expressed on the surface of T-cells. The gene of the IFN-γ receptor α-chain (*IFNGR1*) belongs to housekeeping genes, and the expression of this gene appears to be constitutive [98]. In contrast, the expression of the IFN-γ receptor β chain in certain cell types is regulated by external stimuli. Regulation of the IFN-γ receptor β chain gene is a critical factor in determining IFN-γ responsiveness in certain cells. Overall, both IFN-γ receptors play a critical role in providing innate and adaptive resistance of the host to microbial infections [99-101]. Modifications in the human IFN-γ receptor resulted in a severe susceptibility of hosts to weakly pathogenic mycobacterial species [102, 103]. The IFN-γ receptor α chain knock-out mice (IFN-γ-R$\alpha^{-/-}$) displayed a greatly impaired ability to resist infection caused by a variety of microbial pathogens [99, 101].

We show here that the interaction of LcrV and $LcrV_{68-326}$ with hIFN-γ but not with mIFN-γ induces apoptosis of human Jurkat T-cells and human normal primary thymocytes. These data provide the first conclusive evidence that plague pathogenesis in human and mouse can differ. It should be kept in mind that to objectively assess the protective properties of new anti-plague vaccines for humans in pre-clinical studies, using several model organisms, including mice, is required. We also show that treatment of human T-cells with monoclonal antibodies specific to

the $LEEL_{32-35}$ and $DEEI_{203-206}$ binding sites of LcrV completely blocked the programmed cell death induced by LcrV or $LcrV_{68-326}$.

Apoptosis induction in T-cells is most commonly initiated in response to death receptor ligation, peptideresulting in activation of caspase-8 (extrinsic pathway) [104], or cellular stress followed by mitochondrial release of cytochrome *c* and subsequent activation of caspase-9 (intrinsic pathway) [105]. Apoptosis activation can be a very complex process, making it difficult to specifically implicate a single pathway responsible for the induction of cell death. The molecular mechanisms that initiates apoptosis of human T-cells after LcrV interaction with receptor-bound human IFN-γ will be elucidated in our subsequent studies.

ACKNOWLEDGEMENTS

We would like to thank Alexey Uversky for careful reading and editing of this manuscript.

ABBREVIATIONS

LcrV, V antigen of the plague bacterium *Yersinia pestis*; IL-10, interleukin 10; hIFN-γ, human interferon-γ; hΔIFN-γ, C-terminally truncated form of human interferon-γ; mIFN-γ mouse interferon-γ; Yops, yersiniae outer proteins; IFN-γ R-IFN-γ, interferon-γ bound to its receptor, R-IFN-γ; R-IFN-γ, receptor of interferon-γ

REFERENCES

[1] E. Carniel, [The plague], C R Biol 325(8) (2002) 851-3; discussion 879-83.

[2] M. Achtman, K. Zurth, G. Morelli, G. Torrea, A. Guiyoule, E. Carniel, Yersinia pestis, the

cause of plague, is a recently emerged clone of Yersinia pseudotuberculosis, Proc Natl Acad Sci U S A 96(24) (1999) 14043-8.

[3] P. Hu, J. Elliott, P. McCready, E. Skowronski, J. Garnes, A. Kobayashi, R.R. Brubaker, E. Garcia, Structural organization of virulence-associated plasmids of Yersinia pestis, J Bacteriol 180(19) (1998) 5192-202.

[4] C. Lambert de Rouvroit, C. Sluiters, G.R. Cornelis, Role of the transcriptional activator, VirF, and temperature in the expression of the pYV plasmid genes of Yersinia enterocolitica, Mol Microbiol 6(3) (1992) 395-409.

[5] J.R. Rohde, X.S. Luan, H. Rohde, J.M. Fox, S.A. Minnich, The Yersinia enterocolitica pYV virulence plasmid contains multiple intrinsic DNA bends which melt at 37 degrees C, J Bacteriol 181(14) (1999) 4198-204.

[6] J. Pettersson, R. Nordfelth, E. Dubinina, T. Bergman, M. Gustafsson, K.E. Magnusson, H. Wolf-Watz, Modulation of virulence factor expression by pathogen target cell contact, Science 273(5279) (1996) 1231-3.

[7] R.R. Brubaker, M.J. Surgalla, The Effect of Ca++ and Mg++ on Lysis, Growth, and Production of Virulence Antigens by Pasteurella Pestis, J Infect Dis 114 (1964) 13-25.

[8] H. Smith, J. Keppie, E.C. Cocking, K. Witt, The chemical basis of the virulence of Pasteurella pestis. I. The isolation and the aggressive properties of Past. pestis and its products from infected guinea pigs., Br. J. Exp. Pathol. 41 (1960) 452-459.

[9] R. Nakajima, R.R. Brubaker, Association between virulence of Yersinia pestis and suppression of gamma interferon and tumor necrosis factor alpha, Infect Immun 61(1) (1993) 23-31.

[10] R.R. Brubaker, Interleukin-10 and inhibition of innate immunity to Yersiniae: roles of Yops and LcrV (V antigen), Infect Immun 71(7) (2003) 3673-81.

[11] J. Heesemann, A. Sing, K. Trulzsch, Yersinia's stratagem: targeting innate and adaptive immune defense, Curr Opin Microbiol 9(1) (2006) 55-61.

[12] C.A. Mueller, P. Broz, S.A. Muller, P. Ringler, F. Erne-Brand, I. Sorg, M. Kuhn, A. Engel, G.R. Cornelis, The V-antigen of Yersinia forms a distinct structure at the tip of injectisome needles, Science 310(5748) (2005) 674-6.

[13] G.R. Cornelis, Yersinia type III secretion: send in the effectors, J Cell Biol 158(3) (2002) 401-8.

[14] R. Nakajima, V.L. Motin, R.R. Brubaker, Suppression of cytokines in mice by protein A-V antigen fusion peptide and restoration of synthesis by active immunization, Infect Immun 63(8) (1995) 3021-9.

[15] K. Kawahara, H. Tsukano, H. Watanabe, B. Lindner, M. Matsuura, Modification of the structure and activity of lipid A in Yersinia pestis lipopolysaccharide by growth temperature, Infect Immun 70(8) (2002) 4092-8.

[16] A.K. Sample, R.R. Brubaker, Post-translational regulation of Lcr plasmid-mediated peptides in pesticinogenic Yersinia pestis, Microb Pathog 3(4) (1987) 239-48.

[17] D.M. Monack, J. Mecsas, D. Bouley, S. Falkow, Yersinia-induced apoptosis in vivo aids in the establishment of a systemic infection of mice, J Exp Med 188(11) (1998) 2127-37.

[18] K. Orth, L.E. Palmer, Z.Q. Bao, S. Stewart, A.E. Rudolph, J.B. Bliska, J.E. Dixon, Inhibition of the mitogen-activated protein kinase kinase superfamily by a Yersinia effector, Science 285(5435) (1999) 1920-3.

[19] S. Mukherjee, G. Keitany, Y. Li, Y. Wang, H.L. Ball, E.J. Goldsmith, K. Orth, Yersinia YopJ acetylates and inhibits kinase activation by blocking phosphorylation, Science 312(5777) (2006) 1211-4.

[20] S. Bruckner, S. Rhamouni, L. Tautz, J.B. Denault, A. Alonso, B. Becattini, G.S. Salvesen, T. Mustelin, Yersinia phosphatase induces mitochondrially dependent apoptosis of T cells, J Biol Chem 280(11) (2005) 10388-94.

[21] H. Park, K. Teja, J.J. O'Shea, R.M. Siegel, The Yersinia effector protein YpkA induces apoptosis independently of actin depolymerization, J Immunol 178(10) (2007) 6426-34.

[22] N. Lemaitre, F. Sebbane, D. Long, B.J. Hinnebusch, Yersinia pestis YopJ suppresses tumor necrosis factor alpha induction and contributes to apoptosis of immune cells in the lymph node but is not required for virulence in a rat model of bubonic plague, Infect Immun 74(9) (2006) 5126-31.

[23] T. Une, R.R. Brubaker, Roles of V antigen in promoting virulence and immunity in yersiniae, J Immunol 133(4) (1984) 2226-30.

[24] T. Une, R. Nakajima, R.R. Brubaker, Roles of V antigen in promoting virulence in Yersiniae, Contrib Microbiol Immunol 9 (1987) 179-85.

[25] V.A. Feodorova, L.V. Sayapina, M.J. Corbel, V.L. Motin, Russian vaccines against especially dangerous bacterial pathogens, Emerg Microbes Infect 3(12) (2014) e86.

[26] W.D. Lawton, R.L. Erdman, M.J. Surgalla, Biosynthesis and Purification of V and W Antigen in Pasteurella Pestis, J Immunol 91 (1963) 179-84.

[27] K. Sato, R. Nakajima, F. Hara, T. Une, Y. Osada, Preparation of monoclonal antibody to V antigen from Yersinia pestis, Contrib Microbiol Immunol 12 (1991) 225-9.

[28] V.L. Motin, R. Nakajima, G.B. Smirnov, R.R. Brubaker, Passive immunity to yersiniae mediated by anti-recombinant V antigen and protein A-V antigen fusion peptide, Infect Immun 62(10) (1994) 4192-201.

[29] J. Hill, S.E. Leary, K.F. Griffin, E.D. Williamson, R.W. Titball, Regions of Yersinia pestis V antigen that contribute to protection against plague identified by passive and active immunization, Infect Immun 65(11) (1997) 4476-82.

[30] J. Hill, C. Copse, S. Leary, A.J. Stagg, E.D. Williamson, R.W. Titball, Synergistic protection of mice against plague with monoclonal antibodies specific for the F1 and V antigens of Yersinia pestis, Infect Immun 71(4) (2003) 2234-8.

[31] C. Cowan, A.V. Philipovskiy, C.R. Wulff-Strobel, Z. Ye, S.C. Straley, Anti-LcrV antibody inhibits delivery of Yops by Yersinia pestis KIM5 by directly promoting phagocytosis, Infect Immun 73(9) (2005) 6127-37.

[32] J. Hill, J.E. Eyles, S.J. Elvin, G.D. Healey, R.A. Lukaszewski, R.W. Titball, Administration of antibody to the lung protects mice against pneumonic plague, Infect Immun 74(5) (2006) 3068-70.

[33] S.E. Leary, E.D. Williamson, K.F. Griffin, P. Russell, S.M. Eley, R.W. Titball, Active immunization with recombinant V antigen from Yersinia pestis protects mice against plague, Infect Immun 63(8) (1995) 2854-8.

[34] P. Russell, S.M. Eley, S.E. Hibbs, R.J. Manchee, A.J. Stagg, R.W. Titball, A comparison of Plague vaccine, USP and EV76 vaccine induced protection against Yersinia pestis in a murine model, Vaccine 13(16) (1995) 1551-6.

[35] G.W. Anderson, Jr., S.E. Leary, E.D. Williamson, R.W. Titball, S.L. Welkos, P.L. Worsham, A.M. Friedlander, Recombinant V antigen protects mice against pneumonic and bubonic plague caused by F1-capsule-positive and -negative strains of Yersinia pestis, Infect Immun 64(11) (1996) 4580-5.

[36] V.L. Motin, Y.A. Nedialkov, R.R. Brubaker, V antigen-polyhistidine fusion peptide: binding to LcrH and active immunity against plague, Infect Immun 64(10) (1996) 4313-8.

[37] E.D. Williamson, Plague vaccine research and development, J Appl Microbiol 91(4) (2001) 606-8.

[38] E.D. Williamson, R.W. Titball, Vaccines against dangerous pathogens, Br Med Bull 62 (2002) 163-73.

[39] R.W. Titball, E.D. Williamson, Yersinia pestis (plague) vaccines, Expert Opin Biol Ther 4(6) (2004) 965-73.

[40] K.A. Overheim, R.W. Depaolo, K.L. Debord, E.M. Morrin, D.M. Anderson, N.M. Green, R.R. Brubaker, B. Jabri, O. Schneewind, LcrV plague vaccine with altered immunomodulatory properties, Infect Immun 73(8) (2005) 5152-9.

[41] S.J. Elvin, J.E. Eyles, K.A. Howard, E. Ravichandran, S. Somavarappu, H.O. Alpar, E.D. Williamson, Protection against bubonic and pneumonic plague with a single dose microencapsulated sub-unit vaccine, Vaccine 24(20) (2006) 4433-9.

[42] V.M. Abramov, V.S. Khlebnikov, A.M. Vasiliev, I.V. Kosarev, R.N. Vasilenko, N.L. Kulikova, A.V. Khodyakova, V.I. Evstigneev, V.N. Uversky, V.L. Motin, G.B. Smirnov, R.R. Brubaker, Attachment of LcrV from Yersinia pestis at dual binding sites to human TLR-2 and human IFN-gamma receptor, J Proteome Res 6(6) (2007) 2222-31.

[43] M.J. Finegold, J.J. Petery, R.F. Berendt, H.R. Adams, Studies on the pathogenesis of plague. Blood coagulation and tissue responses of Macaca mulatta following exposure to aerosols of Pasteurella pestis, Am J Pathol 53(1) (1968) 99-114.

[44] J.H. Morrissey, Silver stain for proteins in polyacrylamide gels: a modified procedure with enhanced uniform sensitivity, Anal Biochem 117(2) (1981) 307-10.

[45] M.V. Hobbs, W.O. Weigle, D.J. Noonan, B.E. Torbett, R.J. McEvilly, R.J. Koch, G.J. Cardenas, D.N. Ernst, Patterns of cytokine gene expression by CD4+ T cells from young and old mice, J Immunol 150(8 Pt 1) (1993) 3602-14.

[46] P.R. Salacinski, C. McLean, J.E. Sykes, V.V. Clement-Jones, P.J. Lowry, Iodination of proteins, glycoproteins, and peptides using a solid-phase oxidizing agent, 1,3,4,6-tetrachloro-3 alpha,6 alpha-diphenyl glycoluril (Iodogen), Anal Biochem 117(1) (1981) 136-46.

[47] J.H. Russell, Activation-induced death of mature T cells in the regulation of immune responses, Curr Opin Immunol 7(3) (1995) 382-8.

[48] P. Romero, Z. Obradovic, X. Li, E.C. Garner, C.J. Brown, A.K. Dunker, Sequence complexity of disordered protein, Proteins 42(1) (2001) 38-48.

[49] K. Peng, S. Vucetic, P. Radivojac, C.J. Brown, A.K. Dunker, Z. Obradovic, Optimizing long intrinsic disorder predictors with protein evolutionary information, Journal of bioinformatics and computational biology 3(1) (2005) 35-60.

[50] K. Peng, P. Radivojac, S. Vucetic, A.K. Dunker, Z. Obradovic, Length-dependent prediction of protein intrinsic disorder, BMC bioinformatics 7 (2006) 208.

[51] B. Xue, R.L. Dunbrack, R.W. Williams, A.K. Dunker, V.N. Uversky, PONDR-FIT: a meta-predictor of intrinsically disordered amino acids, Biochimica et biophysica acta 1804(4) (2010) 996-1010.

[52] Z. Dosztanyi, V. Csizmok, P. Tompa, I. Simon, IUPred: web server for the prediction of intrinsically unstructured regions of proteins based on estimated energy content, Bioinformatics 21(16) (2005) 3433-4.

[53] Z.L. Peng, L. Kurgan, Comprehensive comparative assessment of in-silico predictors of disordered regions, Current protein & peptide science 13(1) (2012) 6-18.

[54] X. Fan, L. Kurgan, Accurate prediction of disorder in protein chains with a comprehensive and empirically designed consensus, Journal of biomolecular structure & dynamics 32(3) (2014) 448-64.

[55] Z. Obradovic, K. Peng, S. Vucetic, P. Radivojac, C.J. Brown, A.K. Dunker, Predicting intrinsic disorder from amino acid sequence, Proteins 53 Suppl 6 (2003) 566-72.

[56] A.K. Dunker, J.D. Lawson, C.J. Brown, R.M. Williams, P. Romero, J.S. Oh, C.J. Oldfield, A.M. Campen, C.M. Ratliff, K.W. Hipps, J. Ausio, M.S. Nissen, R. Reeves, C. Kang, C.R. Kissinger, R.W. Bailey, M.D. Griswold, W. Chiu, E.C. Garner, Z. Obradovic, Intrinsically disordered protein, J Mol Graph Model 19(1) (2001) 26-59.

[57] Z. Dosztanyi, V. Csizmok, P. Tompa, I. Simon, The pairwise energy content estimated from amino acid composition discriminates between folded and intrinsically unstructured proteins, J Mol Biol 347(4) (2005) 827-39.

[58] J. Prilusky, C.E. Felder, T. Zeev-Ben-Mordehai, E.H. Rydberg, O. Man, J.S. Beckmann, I. Silman, J.L. Sussman, FoldIndex: a simple tool to predict whether a given protein sequence is intrinsically unfolded, Bioinformatics 21(16) (2005) 3435-8.

[59] A. Campen, R.M. Williams, C.J. Brown, J. Meng, V.N. Uversky, A.K. Dunker, TOP-IDP-scale: a new amino acid scale measuring propensity for intrinsic disorder, Protein Pept Lett 15(9) (2008) 956-63.

[60] P.W. Gray, D.W. Leung, D. Pennica, E. Yelverton, R. Najarian, C.C. Simonsen, R. Derynck, P.J. Sherwood, D.M. Wallace, S.L. Berger, A.D. Levinson, D.V. Goeddel, Expression of human immune interferon cDNA in E. coli and monkey cells, Nature 295(5849) (1982) 503-8.

[61] S.E. Ealick, W.J. Cook, S. Vijay-Kumar, M. Carson, T.L. Nagabhushan, P.P. Trotta, C.E. Bugg, Three-dimensional structure of recombinant human interferon-gamma, Science 252(5006) (1991) 698-702.

[62] M.A. Farrar, R.D. Schreiber, The molecular cell biology of interferon-gamma and its receptor, Annu Rev Immunol 11 (1993) 571-611.

[63] D. Lundell, C. Lunn, D. Dalgarno, J. Fossetta, R. Greenberg, R. Reim, M. Grace, S. Narula, The carboxyl-terminal region of human interferon gamma is important for biological activity: mutagenic and NMR analysis, Protein Eng 4(3) (1991) 335-41.

[64] N.D. Griggs, M.A. Jarpe, J.L. Pace, S.W. Russell, H.M. Johnson, The N-terminus and C-terminus of IFN-gamma are binding domains for cloned soluble IFN-gamma receptor, J Immunol 149(2) (1992) 517-20.

[65] A. Sing, D. Rost, N. Tvardovskaia, A. Roggenkamp, A. Wiedemann, C.J. Kirschning, M. Aepfelbacher, J. Heesemann, Yersinia V-antigen exploits toll-like receptor 2 and CD14 for interleukin 10-mediated immunosuppression, J Exp Med 196(8) (2002) 1017-24.

[66] Y.A. Nedialkov, V.L. Motin, R.R. Brubaker, Resistance to lipopolysaccharide mediated by the Yersinia pestis V antigen-polyhistidine fusion peptide: amplification of interleukin-10, Infect Immun 65(4) (1997) 1196-203.

[67] P.J. Murray, STAT3-mediated anti-inflammatory signalling, Biochem Soc Trans 34(Pt 6) (2006) 1028-31.

[68] P.J. Murray, Understanding and exploiting the endogenous interleukin-10/STAT3-mediated anti-inflammatory response, Curr Opin Pharmacol 6(4) (2006) 379-86.

[69] U. Derewenda, A. Mateja, Y. Devedjiev, K.M. Routzahn, A.G. Evdokimov, Z.S. Derewenda, D.S. Waugh, The structure of Yersinia pestis V-antigen, an essential virulence factor and mediator of immunity against plague, Structure 12(2) (2004) 301-6.

[70] M.R. Walter, W.T. Windsor, T.L. Nagabhushan, D.J. Lundell, C.A. Lunn, P.J. Zauodny, S.K. Narula, Crystal structure of a complex between interferon-gamma and its soluble high-affinity receptor, Nature 376(6537) (1995) 230-5.

[71] D.J. Thiel, M.H. le Du, R.L. Walter, A. D'Arcy, C. Chene, M. Fountoulakis, G. Garotta, F.K. Winkler, S.E. Ealick, Observation of an unexpected third receptor molecule in the crystal structure of human interferon-gamma receptor complex, Structure 8(9) (2000) 927-36.

[72] K. Gunasekaran, C.J. Tsai, R. Nussinov, Analysis of ordered and disordered protein complexes reveals structural features discriminating between stable and unstable monomers, J Mol Biol 341(5) (2004) 1327-41.

[73] C.J. Oldfield, J. Meng, J.Y. Yang, M.Q. Yang, V.N. Uversky, A.K. Dunker, Flexible nets: disorder and induced fit in the associations of p53 and 14-3-3 with their partners, BMC Genomics 9 Suppl 1 (2008) S1.

[74] Z. Wu, G. Hu, J. Yang, Z. Peng, V.N. Uversky, L. Kurgan, In various protein complexes, disordered protomers have large per-residue surface areas and area of protein-, DNA- and RNA-binding interfaces, FEBS Lett 589(19 Pt A) (2015) 2561-9.

[75] A.K. Dunker, C.J. Brown, J.D. Lawson, L.M. Iakoucheva, Z. Obradovic, Intrinsic disorder and protein function, Biochemistry 41(21) (2002) 6573-82.

[76] A.K. Dunker, C.J. Brown, Z. Obradovic, Identification and functions of usefully disordered proteins, Adv Protein Chem 62 (2002) 25-49.

[77] P. Tompa, Intrinsically unstructured proteins, Trends Biochem Sci 27(10) (2002) 527-33.

[78] G.W. Daughdrill, G.J. Pielak, V.N. Uversky, M.S. Cortese, A.K. Dunker, Natively disordered proteins, in: J. Buchner, T. Kiefhaber (Eds.), Handbook of Protein Folding, Wiley-VCH, Verlag GmbH & Co., Weinheim, Germany, 2005, pp. 271-353.

[79] C.J. Oldfield, Y. Cheng, M.S. Cortese, P. Romero, V.N. Uversky, A.K. Dunker, Coupled folding and binding with alpha-helix-forming molecular recognition elements, Biochemistry 44(37) (2005) 12454-70.

[80] P. Radivojac, L.M. Iakoucheva, C.J. Oldfield, Z. Obradovic, V.N. Uversky, A.K. Dunker, Intrinsic disorder and functional proteomics, Biophys J 92(5) (2007) 1439-56.

[81] V.N. Uversky, C.J. Oldfield, A.K. Dunker, Showing your ID: intrinsic disorder as an ID for recognition, regulation and cell signaling, J Mol Recognit 18(5) (2005) 343-84.

[82] A.K. Dunker, I. Silman, V.N. Uversky, J.L. Sussman, Function and structure of inherently disordered proteins, Curr Opin Struct Biol 18(6) (2008) 756-64.

[83] A.K. Dunker, V.N. Uversky, Signal transduction via unstructured protein conduits, Nat Chem Biol 4(4) (2008) 229-30.

[84] V.N. Uversky, A.K. Dunker, Understanding protein non-folding, Biochimica et biophysica acta 1804(6) (2010) 1231-1264.

[85] V.N. Uversky, Multitude of binding modes attainable by intrinsically disordered proteins: a portrait gallery of disorder-based complexes, Chem Soc Rev 40(3) (2011) 1623-34.

[86] V.N. Uversky, Disordered competitive recruiter: fast and foldable, J Mol Biol 418(5) (2012) 267-8.

[87] V.N. Uversky, Intrinsic Disorder-based Protein Interactions and their Modulators, Curr Pharm Des 19(23) (2013) 4191-213.

[88] H.J. Dyson, P.E. Wright, Coupling of folding and binding for unstructured proteins, Curr Opin Struct Biol 12(1) (2002) 54-60.

[89] H.J. Dyson, P.E. Wright, Intrinsically unstructured proteins and their functions, Nat Rev Mol Cell Biol 6(3) (2005) 197-208.

[90] P.E. Wright, H.J. Dyson, Intrinsically unstructured proteins: re-assessing the protein structure-function paradigm, J Mol Biol 293(2) (1999) 321-31.

[91] V.N. Uversky, J.R. Gillespie, A.L. Fink, Why are "natively unfolded" proteins unstructured under physiologic conditions?, Proteins 41(3) (2000) 415-27.

[92] A. Mohan, C.J. Oldfield, P. Radivojac, V. Vacic, M.S. Cortese, A.K. Dunker, V.N. Uversky, Analysis of molecular recognition features (MoRFs), J Mol Biol 362(5) (2006) 1043-59.

[93] V. Vacic, C.J. Oldfield, A. Mohan, P. Radivojac, M.S. Cortese, V.N. Uversky, A.K. Dunker, Characterization of molecular recognition features, MoRFs, and their binding partners, J Proteome Res 6(6) (2007) 2351-66.

[94] V.N. Uversky, Unusual biophysics of intrinsically disordered proteins, Biochimica et biophysica acta 1834(5) (2013) 932-51.

[95] B. Meszaros, I. Simon, Z. Dosztanyi, Prediction of protein binding regions in disordered proteins, PLoS Comput Biol 5(5) (2009) e1000376.

[96] Z. Dosztanyi, B. Meszaros, I. Simon, ANCHOR: web server for predicting protein binding regions in disordered proteins, Bioinformatics 25(20) (2009) 2745-6.

[97] A.A. Nuara, L.J. Walter, N.J. Logsdon, S.I. Yoon, B.C. Jones, J.M. Schriewer, R.M. Buller, M.R. Walter, Structure and mechanism of IFN-gamma antagonism by an orthopoxvirus IFN-gamma-binding protein, Proc Natl Acad Sci U S A 105(6) (2008) 1861-6.

[98] E.A. Bach, M. Aguet, R.D. Schreiber, The IFN gamma receptor: a paradigm for cytokine receptor signaling, Annu Rev Immunol 15 (1997) 563-91.

[99] R. Kamijo, J. Le, D. Shapiro, E.A. Havell, S. Huang, M. Aguet, M. Bosland, J. Vilcek, Mice that lack the interferon-gamma receptor have profoundly altered responses to infection with Bacillus Calmette-Guerin and subsequent challenge with lipopolysaccharide, J Exp Med 178(4) (1993) 1435-40.

[100] S. Huang, W. Hendriks, A. Althage, S. Hemmi, H. Bluethmann, R. Kamijo, J. Vilcek, R.M. Zinkernagel, M. Aguet, Immune response in mice that lack the interferon-gamma receptor, Science 259(5102) (1993) 1742-5.

[101] N.A. Buchmeier, R.D. Schreiber, Requirement of endogenous interferon-gamma production for resolution of Listeria monocytogenes infection, Proc Natl Acad Sci U S A 82(21) (1985) 7404-8.

[102] L. Schejbel, E.M. Rasmussen, H.B. Kemp, A.C. Lundstedt, K.R. Nielsen, N. Obel, H. Marquart, A.B. Andersen, Combined IL-12 receptor and IgA deficiency in an adult man intestinally infested by an unknown, non-cultivable mycobacterium, Scand J Immunol 74(6) (2011) 548-53.

[103] E. Jouanguy, F. Altare, S. Lamhamedi, P. Revy, J.F. Emile, M. Newport, M. Levin, S. Blanche, E. Seboun, A. Fischer, J.L. Casanova, Interferon-gamma-receptor deficiency in an infant with fatal bacille Calmette-Guerin infection, N Engl J Med 335(26) (1996) 1956-61.

[104] N.A. Thornberry, Caspases: key mediators of apoptosis, Chem Biol 5(5) (1998) R97-103.

[105] G.S. Salvesen, Caspases and apoptosis, Essays Biochem 38 (2002) 9-19.

[106] M. Shatsky, R. Nussinov, H.J. Wolfson, A method for simultaneous alignment of multiple protein structures, Proteins 56(1) (2004) 143-56.

[107] W. Humphrey, A. Dalke, K. Schulten, VMD: visual molecular dynamics, J Mol Graph 14(1) (1996) 33-8, 27-8.

Figure Legends

Figure 1. Amino acid sequences of LcrV and target peptides, and primary structures of the C-terminal regions of human and mouse interferons used in the study.

(A) Primary structure of LcrV from *Y. pestis* KIM,[3] where the amino acids of the construct ($LcrV_{68-326}$) first used to prove ability to raise protective antibodies[28] and demonstrate amplification of IL-10 (ref.[66]) are shown in red. Amino acid sequences used to generate synthetic peptides are shown in bold. LEEL and DEEI binding sites responsible for the interaction with receptor-bound hIFN-γ (ref.[42]) are underlined;

(B) Synthetic peptides $LcrV_{31-50}$ containing LEEL binding site and $LcrV_{193-210}$ containing DEEI binding site both responsible for the interaction with receptor-bound hIFN-γ (shown in bold red) are underlined;

(C) Alignment of amino acid sequences of C-terminal regions of human IFN-γ (hIFN-γ), truncated human IFN-γ (hΔIFN-γ), and mouse IFN-γ (mIFN-γ), where identical amino acids are underlined and the GRRA site responsible for the binding LcrV [42] is shown in bold red.

Figure 2. Apoptosis induction in Jurkat T-cells at combined addition of LcrV and human IFN-γ into the culture medium. Staining with propidium iodide. Apoptosis was evaluated by the definition of the events in the hypodiploid peak. Data are from one experiment representative of four independent experiments.

Figure 3. Structural analysis and intrinsic disorder propensity of IFN-γ.

(A) Crystal structure of a complex between the human IFN-γ and the extracellular domain of the IFN-γ receptor α-chain (PDB ID: 1FG9). The two chains that comprise a biologically active IFN-γ homodimer are shown in blue and red. Each IFN-γ monomer contacts one extracellular of

domain IFN-γ receptor α-chain shown as yellow and green surfaces. Red and blue arrows show two opened $GRRA_{138-141}$ sites in the C-terminal regions of IFN-γ homodimer that can be used for the high-affinity specific targeting by LcrV homodimer.

(B) Zoomed in structure of the human IFN-γ homodimer (PDB ID: 1FG9). The two chains that comprise a biologically active IFN-γ homodimer are shown in blue and red. One of the monomers is shown in the translucent form to simplify representation of this highly intertwined homodimer. Red and blue "N" and "C" characters show locations of N- and C-termini of the corresponding monomers.

(C) Evaluation of the intrinsic disorder propensity of the mature form of human IFN-γ (residues 24-166 of UniProt ID: P01579) by a set of commonly utilized disorder predictors, PONDR® VLXT, PONDR® VL3, PONDR® VSL2, PONDR® FIT, IUPred_short, and IUPred_long. Positions of α-helices in the protein are shown by cyan bars. Light pink shadow around PONDR® FIT curve shows distribution of errors.

(D) Multiple structural alignment of crystal structures of human IFN-γ alone (blue structure, PDB ID: 1HIG) [61], or in complex with two extracellular domains of soluble IFN-γ receptor α-chains (red structure, PDB ID: 1FG9) [70, 71], or complexed with the IFN-γ-binding protein from Ectromelia virus (ECTV) (green structure, $IFN\text{-}\gamma BP_{ECTV}$; PDB ID: 3BES) [97]. Multiple structural alignment was conducted using MultiProt web server (http://bioinfo3d.cs.tau.ac.il/MultiProt/) [106]. Structures were visualized using the Visual Molecular Dynamics VMD 1.8.7 package [107].

Table 1. Protein- protein interaction studies of LcrV and $LcrV_{68-326}$ with human IFN-γ and human ΔIFN-γ.

Radioactive protein in solution	Protein immobilized on plastic plates	Dissociation constant, (M)
^{125}I- LcrV	hIFN-γ*	$\geq 10^{-1}$
^{125}I- $LcrV_{68-326}$	hIFN-γ*	$\geq 10^{-1}$
^{125}I- LcrV	hΔIFN-γ*	$\geq 10^{-1}$
^{125}I- $LcrV_{68-326}$	hΔIFN-γ*	$\geq 10^{-1}$
^{125}I- hIFN-γ	LcrV**	$\geq 10^{-1}$
^{125}I- hIFN-γ	$LcrV_{68-326}$**	$\geq 10^{-1}$
^{125}I- hΔ IFN-γ	LcrV**	$\geq 10^{-1}$
^{125}I- hΔIFN-γ	$LcrV_{68-326}$**	$\geq 10^{-1}$
Controls		
^{125}I- LcrV	PABs against LcrV	$(3.6\pm0,4)\times10^{-7}$
^{125}I- $LcrV_{68-326}$	PABs against $LcrV_{68-326}$	$(4.2\pm0.3)\times10^{-7}$
^{125}I- hIFN-γ	PABs against hIFN-γ	$(1.6\pm0.2)\times10^{-8}$
^{125}I- hΔIFN-γ	PABs against hIFN-γ	$(2.8\pm0.5)\times10^{-8}$

* Absorption of hIFN-γ or hΔIFN-γ and

** Absorption of LcrV or $LcrV_{68-326}$ on the plastic plate surface were controlled by FITC-labeled polyclonal rabbit anti h IFN-γ, anti- LcrV, anti- $LcrV_{68-326}$ antibodies (PABs).

Table 2. Specific binding of radioactive LcrV and $LcrV_{68-326}$ in the presence of human IFN-γ and human ΔIFN-γ to Jurkat cells.

Ligand	Dissociation constant, (M)
^{125}I- LcrV	$\geq 10^{-3}$
^{125}I- $LcrV_{68-326}$	$\geq 10^{-3}$
^{125}I- LcrV + hIFN-γ	$(5.2\pm0.3)\times10^{-10}$
^{125}I- $LcrV_{68-326}$ + hIFN-γ	$(4.6\pm0.4)\times10^{-10}$
^{125}I- LcrV + hΔIFN-γ [a]	$\geq 10^{-3}$
^{125}I- $LcrV_{68-326}$ + hΔIFN-γ	$\geq 10^{-3}$
^{125}I- LcrV + hIFN-γ + Anti- LcrV MABs [b]	$\geq 10^{-3}$
^{125}I- $LcrV_{68-326}$ + hIFN-γ + Anti- LcrV MABs	$\geq 10^{-3}$
Controls	
^{125}I- hIFN-γ	$(3.6\pm0.5)\times10^{-10}$
^{125}I- hΔIFN-γ	$(7.8\pm0.4)\times10^{-10}$

[a] Human ΔIFN-γ lacking the first six C-terminal amino acids.

[b] Mouse monoclonal antibodies against peptide $LcrV_{31-50}$ containing binding site LEEL and peptide $LcrV_{193-210}$ containing binding site DEEI (these sites are responsible for the interaction with h IFN-γ).

Table 3. Specific binding of radioactive LcrV in the presence of human IFN-γ, human ΔIFN-γ, human IFN-α2, and mouse IFN-γ to human thymocytes.

Ligand	Dissociation constant, (M)
^{125}I- LcrV	$\geq 10^{-3}$
^{125}I- LcrV + hIFN-γ	$(2.7\pm0.6)\times10^{-10}$
^{125}I- LcrV+ hΔIFN-γ [a]	$\geq 10^{-3}$
^{125}I- LcrV+ hIFN-α2	$\geq 10^{-3}$
^{125}I- LcrV+ mIFN-γ	$\geq 10^{-3}$
^{125}I- LcrV + hIFN-γ + Anti- LcrV MABs [b]	$\geq 10^{-3}$
Controls	
^{125}I- h IFN-γ	$(4.8\pm0.3)\times10^{-10}$
^{125}I- hΔIFN-γ	$(6.7\pm0.5)\times10^{-10}$
^{125}I- hIFN- α2	$(5.0\pm0.4)\times10^{-10}$
^{125}I- mIFN-γ	$(2.9\pm0.2)\times10^{-9}$

[a] Human ΔIFN-γ lacking the first six C-terminal amino acids.
[b] Mouse monoclonal antibodies against peptide $LcrV_{31-50}$ containing binding site LEEL and peptide $LcrV_{193-210}$ containing binding site DEEI (these sites are responsible for the interaction with hIFN-γ).

Table 4. Specific binding of radioactive $LcrV_{68-326}$ in the presence of human IFN-γ, human ΔIFN-γ, human IFN-α2, and mouse IFN-γ to human thymocytes.

Ligand	Dissociation constant, (M)
^{125}I- $LcrV_{68-326}$	$\geq 10^{-3}$
^{125}I- $LcrV_{68-326}$ + hIFN-γ	$(3.5\pm0.4)\times10^{-10}$
^{125}I- $LcrV_{68-326}$ + hΔIFN-γ [a]	$\geq 10^{-3}$
^{125}I- $LcrV_{68-326}$ + hIFN-α2	$\geq 10^{-3}$
^{125}I- $LcrV_{68-326}$ + mIFN-γ	$\geq 10^{-3}$
^{125}I- $LcrV_{68-326}$ + hIFN-γ + Anti- LcrV MAB [b]	$\geq 10^{-3}$

[a] Human ΔIFN-γ lacking the first six C-terminal amino acids.
[b] Mouse monoclonal antibody against peptide $LcrV_{193-210}$ containing binding site DEEI responsible for the interaction with h IFN-γ.

Table 5. Flow cytometric analysis of apoptosis induction in human thymocytes by combined insertion of LcrV and IFN-γ into the culture medium.

Preparation, (μg/ml)	Hypodiploid peak (%)	Diploid peak (%)	Proliferation (%)
Control [a]	5.2±0.6	79.2±1.1	13.7±0.9
LcrV (1.0)	5.7±0.7	82.0±1.4	11.0±0.5
LcrV (10.0)	8.2±0.5	85.8±0.9	6.7±0.3
hIFN-γ (10.0)	6.0±0.8	88.0±1.7	3.9±0.4
LcrV (1.0) + hIFN-γ (10.0)	45.7±1.3**	50.0±0.7	2.2±0.6
LcrV (10.0) + hIFN-γ (10.0)	50.4±1.5**	45.4±0.6	2.5±0.2
LcrV (10.0) + hΔIFN-γ (10,0)	5.3±0.4	85.5±1.2	6.3±0.8
LcrV (10.0) + hIFN-γ (10.0) + Anti-LcrV MABs [b]	6.4±0.8	88.7±1.5	3.8±0.5

Apoptosis was evaluated by the definition of the percentage of hypodiploid cells.
** Differences are authentic ($p<0.01$) on comparative data according to Student. The media ± SD of four independent experiments is shown;
[a] Intact thymocytes;
[b] Mouse monoclonal antibodies against peptide $LcrV_{31-50}$ containing binding site LEEL and peptide $LcrV_{193-210}$ containing binding site DEEI (these sites are responsible for the interaction with h IFN-γ).

Table 6. Flow cytometric analysis of apoptosis induction in human thymocytes by combined insertion of $LcrV_{68-326}$ and IFN-γ into the culture medium.

Preparation, (μg/ml)	Hypodiploid peak (%)	Diploid peak (%)	Proliferation (%)
Control [a]	5.4±0.5	78.6±0.9	14.6±1.1
$LcrV_{68-326}$ (1.0)	5.9±0.6	78.4±1.2	12.5±0.8
$LcrV_{68-326}$ (10.0)	7.4±0.7	83.5±1.3	7.6±0.9
hIFN-γ (10.0)	6.8±0.5	87.6±1.5	4.5±0.6
$LcrV_{68-326}$ (1.0) + hIFN-γ (10.0)	46.4±1.7**	49.2±0.8	2.8±0.3
$LcrV_{68-326}$ (10.0) + hIFN-γ (10.0)	52.8±1.5**	42.5±0.7	3.4±0.2
$LcrV_{68-326}$ (10.0) + hΔIFN-γ (10.0)	7.8±0.5	87.2±1.4	3.3±0.4
$LcrV_{68-326}$ (10.0) + hIFN-γ (10.0) + Anti- LcrV MAB [b]	6.5±0.7	86.1±1.1	4.3±0.5

Apoptosis was evaluated by the definition of the percentage of hypodiploid cells.
** Differences are authentic ($p<0.01$) on comparative data according to Student. The media ± SD of four independent experiments is shown;
[a] Intact thymocytes;
[b] Mouse monoclonal antibody against peptide $LcrV_{193-210}$ containing binding site DEEI responsible for the interaction with h IFN-γ.

AUTHOR INFORMATION

Corresponding Author

* VNU, Department of Molecular Medicine, University of South Florida, 12901 Bruce B. Downs Blvd. MDC07, Tampa, Florida 33612, USA, E-mail: vuversky@health.usf.edu

Author Contributions

The manuscript was written through contributions of all authors. All authors have given approval to the final version of the manuscript.

A

```
>sp|P0C7U7|LCRV_YERPE Virulence-associated V antigen
OS=Yersinia pestis OX=632 GN=lcrV PE=1 SV=1

  1 MIRAYEQNPQ HFIEDLEKVR VEQLTGHGSS VLEELVQLVK DKNIDISIKYD PRKDSEVFA
 61 NRVITDDIEL LKKILAYFLP EDAILKGGHY DNQLQNGIKR VKEFLESSPNT QWELRAFMA
121 VMHFSLTADR IDDDILKVIV DSMNHHGDAR SKLREELAEL TAELKIYSVIQ AEINKHLSS
181 SGTINIHDKS INLMDKNLYG YTDEEIFKAS AEYKILEKMP QTTIQVDGSEK KIVSIKDFL
241 GSENKRTGAL GNLKNSYSYN KDNNELSHFA TTCSDKSRPL NDLVSQKTTQL SDITSRFNS
301 AIEALNRFIQ KYDSVMQRLL DDTSGK
```

B

```
 31  VLEELVQLVKDKNIDISIKY 50
191  LMDKNLYGYTDEEIFKAS   210
```

C

```
.........111.......121.......131.......141.
hIFN-γ     HELIQVMAELSPAAKTGKRKRSQMLFRGRRASQ
hΔIFN-γ    HELIQVMAELSPAAKTGKRKRSQMLFR
mIFN-γ     NELIRVVHQLLPESSLRKRKRSRC
```

Figure 1

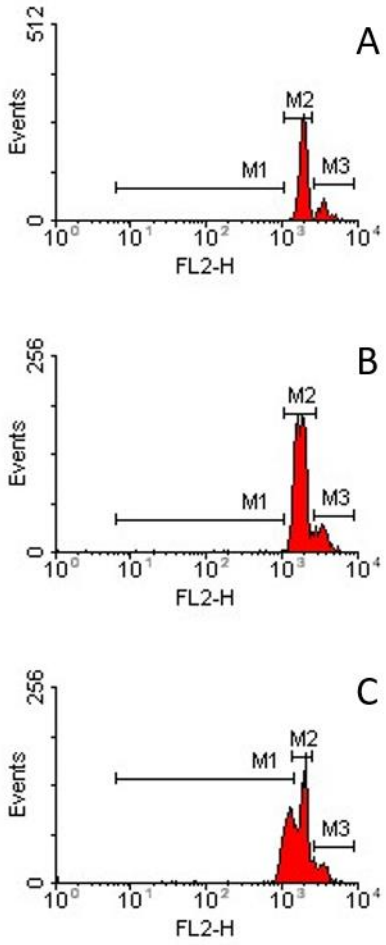

Figure 2

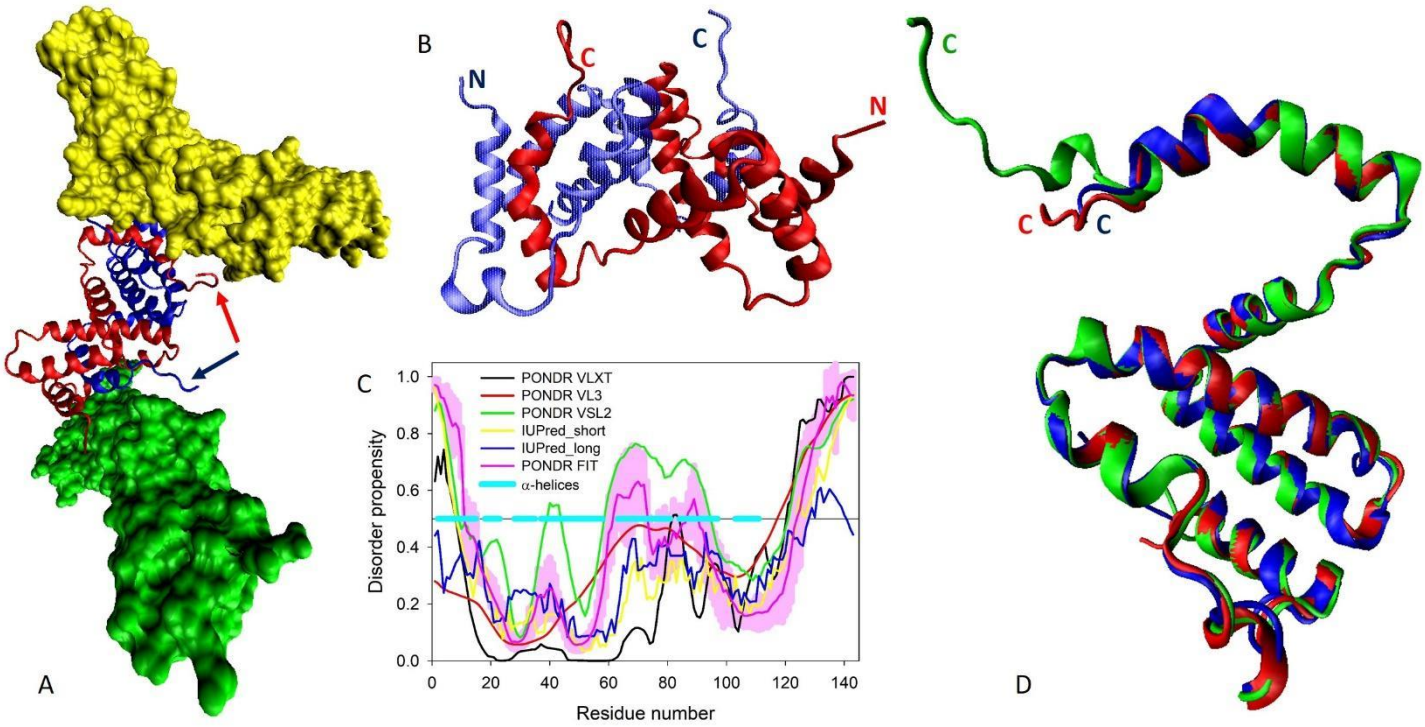

Figure 3